

# A Two-Dimensional Oxamate- and Oxalate-Bridged Cu<sup>II</sup>Mn<sup>II</sup> Motif: Crystal Structure and Magnetic Properties of (Bu<sub>4</sub>N)<sub>2</sub>[Mn<sub>2</sub>{Cu(opba)}<sub>2</sub>ox]

Maria V. Marinho,<sup>†</sup> Tatiana R. G. Simões,<sup>‡</sup> Marcos A. Ribeiro,<sup>‡,§</sup> Cynthia L. M. Pereira,<sup>‡</sup> Flávia C. Machado,<sup>‡</sup> Carlos B. Pinheiro,<sup>§</sup> Humberto O. Stumpf,<sup>\*,‡</sup> Joan Cano,<sup>†,||</sup> Francesc Lloret,<sup>†</sup> and Miguel Julve<sup>\*,†</sup>

<sup>†</sup>Departament de Química Inorgànica/Institut de Ciència Molecular, Facultat de Química de la Universitat de València, C/Catedrático José Beltrán 2, 46980-Paterna (València), Spain

<sup>‡</sup>Departamento de Química, ICEX, Universidade Federal de Minas Gerais, Av. Antônio Carlos 6627, Belo Horizonte-MG 31270-901, Brazil

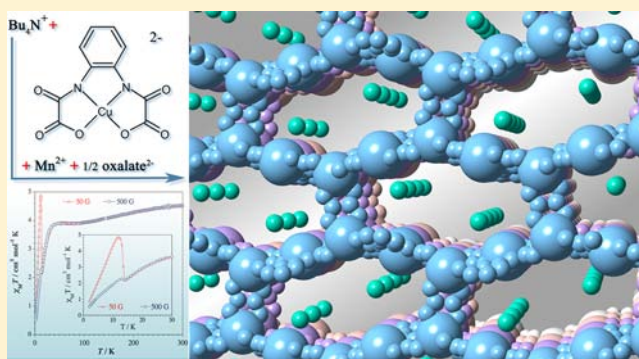
<sup>§</sup>Departamento de Física, ICEX, Universidade Federal de Minas Gerais, av. Antônio Carlos 6627, Belo Horizonte-MG 31270-901, Brazil

<sup>‡</sup>Departamento de Química, ICE, Universidade Federal de Juiz de Fora, 36036-330 Juiz de Fora, Minas Gerais, Brazil

<sup>||</sup>Fundació General de La Universitat de València (FGUV), Universitat de València, 46980 Paterna (València), Spain

## S Supporting Information

**ABSTRACT:** A new compound of formula (Bu<sub>4</sub>N)<sub>2</sub>[Mn<sub>2</sub>{Cu(opba)}<sub>2</sub>ox] (**1**) [Bu<sub>4</sub>N<sup>+</sup> = tetra-*n*-butylammonium cation, H<sub>4</sub>opba = 1,2-phenylenebis(oxamic acid), and H<sub>2</sub>ox = oxalic acid] has been synthesized and magneto-structurally investigated. The reaction of manganese(II) acetate, [Cu(opba)]<sup>2-</sup>, and ox<sup>2-</sup> in dimethyl sulfoxide yielded single crystals of **1**. The structure of **1** consists of heterobimetallic oxamato-bridged Cu<sup>II</sup>Mn<sup>II</sup> chains which are connected through bis-bidentate oxalate coordinated to the manganese(II) ions to afford anionic heterobimetallic layers of 6<sup>3</sup>-hcb net topology. The layers are interleaved by *n*-Bu<sub>4</sub>N<sup>+</sup> counterions. Each copper(II) ion in **1** is four-coordinate in a square planar environment defined by two amidate-nitrogen and two carboxylate-oxygen atoms from the two oxamate groups of the opba ligand. The manganese(II) ion is six-coordinate in a somewhat distorted octahedral surrounding that is built by two oxalate-oxygen and four carbonyl-oxygen atoms from two [Cu(opba)]<sup>2-</sup> units. The magnetic properties of **1** in the temperature range 1.9–300 K correspond to those expected for the coexistence of intralayer antiferromagnetic interactions of the type copper(II)–manganese(II) across oxamato and manganese(II)–manganese(II) through oxalato bridges plus a weak spin canting in the very low temperature domain. Simulation of the magnetic data through quantum Monte Carlo methodology reveals the magnitude of the intralayer magnetic interactions [ $J_{\text{CuMn}} = -32.5(3) \text{ cm}^{-1}$ , and  $J_{\text{MnMn}} = -2.7(3) \text{ cm}^{-1}$ ], their values being within the range of those previously observed in lower nuclearity systems.



## INTRODUCTION

The oxamato/oxamidato-based ligands chemistry is a well-known strategy to design and synthesize multimetallic coordination architectures where the programmed self-assembly of functionalized paramagnetic precursors has provided a plethora of *n*D (*n* = 0–3) magnetic materials.<sup>1–3</sup> Several factors make this strategy one of the safest ones aimed at preparing nuclearity-controlled heterometallic multifunctional compounds: (i) the high stability of the oxamidato- and oxamato-containing copper(II) complexes in solution,<sup>4</sup> (ii) the good and predictable coordinating ability of these copper(II) precursors toward fully solvated metal ions or metal complexes

whose coordination sphere is unsaturated,<sup>5–12</sup> (iii) remarkable ability of the oxamato/oxamidato to mediate magnetic interactions between the paramagnetic centers when acting as a bridge,<sup>13</sup> and (iv) the practically limitless possibilities of the precursor functionalization by the insertion of substituents on the amide nitrogen atoms from the oxamidate or oxamate (chirality, porosity, conductivity, and photosensitivity or redox-

Received: April 25, 2013

Revised: June 24, 2013

Accepted: July 5, 2013

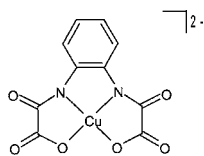
Published: July 15, 2013

sensitivity, for instance) that would allow the chemist to program the preparative work toward the design of multifunctional molecule-based magnetic materials (MMMMs).<sup>14</sup>

With the focus on heterobimetallic one-dimensional compounds, because the pioneering work carried out by Kahn and co-workers demonstrated the feasibility of getting spontaneous magnetization by interchain assembling in the first example of a linear oxamato-bridged manganese(II)–copper(II) ferrimagnetic chain,<sup>15</sup> other oxamato-bridged Cu<sup>II</sup>M<sup>II</sup> (M = Mn and Co) chains with linear, zigzag, or helical structures behaving as almost ideal ferrimagnetic one-dimensional compounds have been prepared and magneto-structurally investigated.<sup>5,11a,g,14b,c,16–18</sup> Interestingly, Cu<sup>II</sup>Co<sup>II</sup> ferrimagnetic chains exhibit slow magnetic relaxation at low temperatures, being examples of single chain magnets (SCMs).<sup>14b,c,18</sup> This SCM behavior obeys the large intrachain Ising-type magnetic anisotropy and minimization of the interchain contacts that arise from the combination of an orbitally degenerate octahedral high-spin cobalt(II) ion (<sup>4</sup>T<sub>1</sub> ground term) and a square planar copper(II) complex with bulky substituents on the oxamate-nitrogen.

Previous magneto-structural studies based on the use of the [Cu(opba)]<sup>2-</sup> (opba = 1,2-phenylenebis(oxamate)) (see Scheme 1) as a ligand toward transition and rare earth cations

**Scheme 1. Structural Drawing of the 1,2-Phenylenebis(oxamato)cuprate(II)**



have shown the possibility of designing linear and zigzag chains,<sup>9,11a,16d,17,19</sup> 2-D networks with honeycomb-<sup>11a,c,e,20,21</sup> and ladder-like<sup>22–24</sup> structures, and 3-D motifs with an interlocked structure.<sup>11b,d</sup>

Here, we show for the first time how the partial hydrolysis of the [Cu(opba)]<sup>2-</sup> precursor in the presence of manganese(III) acetate yields the oxalate anion that acts as linker of the oxamato-bridged Mn<sup>II</sup>Cu<sup>II</sup> zigzag chains in the honeycomb-layered compound of formula (Bu<sub>4</sub>N)<sub>2</sub>[Mn<sub>2</sub>{Cu(opba)}<sub>2</sub>ox] (**1**) (*n*-Bu<sub>4</sub>N<sup>+</sup> = tetra-*n*-butylammonium cation, and ox<sup>2-</sup> = oxalate anion). This hydrolytic reaction produces single crystals of **1** whose structure and magnetic properties are the subject of the present work.

## EXPERIMENTAL SECTION

**Materials.** Manganese(III) acetate dihydrate [Mn(CH<sub>3</sub>COO)<sub>3</sub>·2H<sub>2</sub>O, 97%], manganese(II) acetate tetrahydrate [Mn(CH<sub>3</sub>COO)<sub>2</sub>·4H<sub>2</sub>O, 99%], tetrabutylammonium hydroxide solution [40% in water], and dimethyl sulfoxide [(CH<sub>3</sub>)<sub>2</sub>SO, 99.9%] were purchased from Sigma-Aldrich. Oxalic acid dihydrate [H<sub>2</sub>C<sub>2</sub>O<sub>4</sub>·2H<sub>2</sub>O, 99.5%] were purchased from Cinética Química. The mononuclear copper(II) complex of formula (Bu<sub>4</sub>N)<sub>2</sub>[Cu(opba)] was prepared according to a previously reported procedure.<sup>11a</sup> The (Bu<sub>4</sub>N)<sub>2</sub>ox salt was synthesized as follows: (Bu<sub>4</sub>N)OH (6.5 cm<sup>3</sup>, 40% solution in water, 10.0 mmol) was poured into an aqueous solution of oxalic acid (630 mg, 5.00 mmol) under continuous stirring for 30 min; the removal of the solvent in a rotator evaporator afforded the desired salt as a yellow oil.

**Synthesis of (Bu<sub>4</sub>N)<sub>2</sub>[Mn<sub>2</sub>{Cu(opba)}<sub>2</sub>ox] (**1**).** Mn-(CH<sub>3</sub>COO)<sub>3</sub>·2H<sub>2</sub>O (3.35 mg, 0.012 mmol) dissolved in DMSO (2 cm<sup>3</sup>) was added to another DMSO solution (2 cm<sup>3</sup>) of (Bu<sub>4</sub>N)<sub>2</sub>[Cu(opba)] (50 mg, 0.063 mmol) with stirring at room temperature. A small amount of well-shaped blue crystals were grown on standing for 1 week. They were separated by filtration, washed with a small amount of DMSO, and identified as the bimetallic chain [MnCu(opba)-(DMSO)<sub>3</sub>]<sub>n</sub>.<sup>11a</sup> The resulting violet mother liquor was allowed to stand at room temperature. X-ray-quality crystals of **1** as violet parallelepipeds were collected after 3 months, with the yield being less than 10%. This compound was obtained in a practically quantitative yield by the reaction of Mn-(CH<sub>3</sub>COO)<sub>2</sub>·4H<sub>2</sub>O, (Bu<sub>4</sub>N)<sub>2</sub>[Cu(opba)], and [(Bu<sub>4</sub>N)<sub>2</sub>ox]: an aqueous solution (25 cm<sup>3</sup>) of Mn(CH<sub>3</sub>COO)<sub>2</sub>·4H<sub>2</sub>O (69 mg, 0.282 mmol) was added to a mixture of (Bu<sub>4</sub>N)<sub>2</sub>[Cu(opba)] (228 mg, 0.286 mmol) and [(Bu<sub>4</sub>N)<sub>2</sub>ox] (150 mg, 0.262 mmol) in a solution of DMSO (25 cm<sup>3</sup>) under continuous stirring. Compound **1** was separated as a polycrystalline solid on standing after 1 month. The solid was collected by filtration, washed with DMSO, and dried under a vacuum. Its powder X-ray diffraction pattern (Supporting Information Figure Figure S1) matches the simulated one for the single crystal X-ray structure of **1**; this feature unambiguously supports the identical nature of both products. Anal. Calcd for C<sub>54</sub>H<sub>80</sub>Cu<sub>2</sub>Mn<sub>2</sub>N<sub>6</sub>O<sub>16</sub> (**1**): C, 49.65; H, 6.17; N, 6.43. Found: C, 49.23; H, 6.40; N, 6.60. Cu:Mn molar ratio (electron probe X-ray microanalysis): 1:1.

**Physical Measurements.** Elemental analyses (C, H, N) were performed with a PerkinElmer 2400 analyzer. A value of 1:1 for the Cu:Mn molar ratio was determined through electron probe X-ray microanalysis by using a Philips XL-30 scanning electron microscope (SEM) from the Central Service for Support to Experimental Research (SCSIE) at the University of València. The thermal study (TG/DTA) of a polycrystalline sample of **1** was carried out on a Shimadzu TG-60 thermal analyzer by using 3.23 mg of product packed in an alumina crucible. The sample was heated at 10 °C min<sup>-1</sup> from room temperature to 800 °C in a dynamic dinitrogen atmosphere (flow rate = 100 cm<sup>3</sup> min<sup>-1</sup>). The IR spectrum of **1** was recorded on a Bomen Michelson 102 FTIR spectrophotometer using KBr pellets in the range 4000–400 cm<sup>-1</sup> with an average of 128 scans and 4 cm<sup>-1</sup> of spectral resolution. The polycrystalline sample **1** obtained by the direct method was verified by powder X-ray diffraction (PXRD) measurements performed on a Rigaku setup, in  $\theta$ - $2\theta$  geometry using a copper X-ray emission tube. Magnetic susceptibility measurements of **1** as a polycrystalline sample were carried out on a Quantum Design SQUID magnetometer in the temperature range 1.9–300 K under applied dc fields of 3000 G (50 ≤ *T* ≤ 300 K), 500 G (1.9 ≤ *T* ≤ 50 K), and 50 G (*T* ≤ 30 K). The corrections for the diamagnetism of the constituent atoms of **1** were estimated from Pascal's constants<sup>25</sup> as  $-321 \times 10^{-6}$  cm<sup>3</sup> mol<sup>-1</sup> per Cu<sup>II</sup>Mn<sup>II</sup> pair. Corrections for the temperature-independent paramagnetism [ $60 \times 10^{-6}$  cm<sup>3</sup> mol<sup>-1</sup> per Cu<sup>II</sup>] and the sample holder were also applied.

**Computational Details.** Quantum Monte Carlo (QMC) simulations were carried out by using the decoupled cell method (DCM), described elsewhere, in which the probability of a spin flip is calculated from the exact solution of a model that is made up of this spin and the first and second neighbors.<sup>26</sup> The network model was built from the 12 × 6 repetition of a cell with eight (2 × 4) sites by imposing periodic

boundary conditions. In order to avoid freezing of the spin configuration, we have used a low cooling rate according to the following expression:  $T_{i+1} = 0.98T_i$ . The number of Monte Carlo steps per site at each temperature was 50 000, and 10% were used in the thermalization process. The probability of a spin flip of a center was calculated from an exact diagonalization of the energy matrix of a system involving this center and the first and second neighbors. Thus, these systems are constituted by eight and seven sites for the  $S = 5/2$  and  $S = 1/2$  local spin moments. From the spin-flip probabilities and using a metropolis algorithm, a sampling was generated where the states more present are those that have a more important contribution in the partition function. This sampling allowed us to calculate the average magnetization at a given temperature, and the molar magnetic susceptibility was obtained from the fluctuations in the magnetization through eq 1

$$\chi_M T = N\beta^2/k(\langle \mathbf{M}^2 \rangle - \langle \mathbf{M} \rangle^2) \quad (1)$$

where  $\langle \mathbf{M} \rangle$  and  $\langle \mathbf{M} \rangle^2$  are the mean values of the magnetization and its square and  $N$ ,  $\beta$ , and  $k$  have their usual meaning.

The size of the small systems used to calculate the spin-flip probabilities limits the quality of these simulations at low temperature in this approach. Moreover, the simulations in this study only could be applied for  $T/J_{\text{CuMn}} \geq 0.6$ . In order to study magnetic behaviors at lower temperatures, larger systems as a base for spin-flip probabilities or a more powerful method, such as the modified decoupled cell (mDCM), should be used.<sup>27</sup> However, it was not done herein because of the occurrence of a spin-canting phenomenon at low temperatures.

**X-ray Data Collection and Structure Refinement.** X-ray data for a single crystal of **1** with dimensions  $0.31 \times 0.09 \times 0.04$  mm were collected on an Oxford-Diffraction GEMINI diffractometer by using graphite-monochromated Cu  $K\alpha$  radiation ( $\lambda = 1.5418 \text{ \AA}$ ) at 120(2) K. Accurate unit cell dimensions and orientation matrices were determined by least-squares refinement of the reflections obtained by  $\theta$ - $\chi$  scans. The data were indexed and scaled with the *CrysalisPro* program.<sup>28</sup> Analytical absorption corrections of the diffracted intensities based on a multifaceted crystal model using *CrysalisPro*<sup>28</sup> were applied to **1**. The indexes of the data collection were  $-11 \leq h \leq 10$ ,  $-19 \leq k \leq 19$ , and  $-21 \leq l \leq 21$ . Of the 36 943 measured independent reflections in the  $3.6$ – $66.1^\circ$   $\theta$  range, 5073 were considered independent and observed [ $I \geq 2.0\sigma(I)$ ] and 4034 were reflections. The crystal structure of **1** was solved by direct methods using the *SHELX-97* package.<sup>29</sup> The structure was refined by a full-matrix least-squares technique on  $F^2$  using the *SHELX-97* programs.<sup>29</sup> All non-hydrogen atoms in **1** were refined anisotropically. The hydrogen atoms in the compound were added to the structure in idealized positions and further refined according to the riding model.<sup>30</sup> The final geometric calculations were carried out with *PLATON*,<sup>31</sup> whereas the graphical manipulations were performed with the *DIAMOND*,<sup>32a</sup> *Mercury*,<sup>32b</sup> and *ORTEP*<sup>30</sup> programs. A summary of the crystal data and refinement conditions for **1** is given in Table 1, and selected bond lengths and angles are listed in Table 2.

## RESULTS AND DISCUSSION

### Synthesis, IR Characterization, and Thermal Study of

**1.** Compound **1** was synthesized using the  $[\text{Cu}(\text{opba})]^{2-}$  building block as a ligand toward the  $\text{Mn}^{3+}$  ions in DMSO solution. The partial hydrolysis of the oxamate groups of the

**Table 1.** Summary of the Crystal Data and Refinement Details for **1**

compound	<b>1</b>
formula	$\text{C}_{27}\text{H}_{40}\text{CuMnN}_3\text{O}_8$
crystal size/mm <sup>3</sup>	$0.31 \times 0.09 \times 0.04$
fw	653.1
crystal system	monoclinic
space group	$P2_1/n$
$a/\text{\AA}$	9.7093 (8)
$b/\text{\AA}$	16.5851 (17)
$c/\text{\AA}$	18.1758 (15)
$\beta/\text{deg}$	90.500 (7)
$V/\text{\AA}^3$	2926.7 (5)
$Z$	4
$\lambda/\text{\AA}$	1.5418
$\rho/\text{mg m}^{-3}$	1.482
$T/\text{K}$	120(2)
$\lambda(\text{Cu } K\alpha)/\text{mm}^{-1}$	4.84
no. of parameters	365
goodness-of-fit on $F^2$	1.04
$R^a$ , $wR^b$ [ $I > 2\sigma(I)$ ]	0.046, 0.120
$R^a$ , $wR^b$ (all data)	0.0639, 0.1197
largest diffraction peak and hole/e $\text{\AA}^{-3}$	1.56, $-0.40$

$$^a R = \sum \|F_o\| - \|F_c\| / \sum \|F_o\|, \quad ^b wR = [\sum (|F_o|^2 - |F_c|^2)^2 / \sum |F_o|^2]^{1/2}.$$

**Table 2.** Selected Bond Distances ( $\text{\AA}$ ) and Angles ( $\text{deg}$ ) for **1**<sup>a</sup>

Cu1—N2	1.915 (3)	Mn1—O2	2.184 (2)
Cu1—N1	1.917 (3)	Mn1—O3	2.193 (2)
Cu1—O4	1.942 (2)	Mn1—O5 <sup>i</sup>	2.195 (2)
Cu1—O1	1.960 (2)	Mn1—O6 <sup>i</sup>	2.211 (2)
Mn1—O7	2.152 (2)	O6—Mn1 <sup>ii</sup>	2.211 (2)
Mn1—O8	2.183 (3)	O5—Mn1 <sup>ii</sup>	2.195 (2)
N2—Cu1—N1	83.92 (11)	O2—Mn1—O3	76.71 (8)
N2—Cu1—O4	85.39 (10)	O7—Mn1—O5 <sup>i</sup>	93.48 (9)
N1—Cu1—O4	169.29 (11)	O8—Mn1—O5 <sup>i</sup>	91.96 (9)
N2—Cu1—O1	168.84 (11)	O2—Mn1—O5 <sup>i</sup>	84.90 (9)
N1—Cu1—O1	85.12 (10)	O3—Mn1—O5 <sup>i</sup>	160.80 (10)
O4—Cu1—O1	105.53 (10)	O7—Mn1—O6 <sup>i</sup>	84.86 (9)
O7—Mn1—O8	76.96 (9)	O8—Mn1—O6 <sup>i</sup>	157.93 (9)
O7—Mn1—O2	166.25 (9)	O2—Mn1—O6 <sup>i</sup>	107.93 (9)
O8—Mn1—O2	89.43 (9)	O3—Mn1—O6 <sup>i</sup>	103.69 (9)
O7—Mn1—O3	105.69 (9)	O5 <sup>i</sup> —Mn1—O6 <sup>i</sup>	76.58 (9)
O8—Mn1—O3	93.32 (9)		

<sup>a</sup>Symmetry codes: (i)  $x - 1/2, -y + 1/2, z - 1/2$ . (ii)  $x + 1/2, -y + 1/2, z + 1/2$ .

opba ligand affording the oxalate dianion, together with the reduction of  $\text{Mn}^{\text{III}}$  to  $\text{Mn}^{\text{II}}$ , accounts for the formation of single crystals of **1**. This hydrolytic reaction of the oxamate (or the related oxamidate) to yield oxalate has been observed by different authors in previous magneto-structural studies either under ambient<sup>4,13a,33</sup> or hydrothermal conditions.<sup>34</sup> This hydrolytic process provided X-ray quality crystals of **1** in a very low yield. Here, once the formula of this compound was established by single crystal X-ray diffraction, we prepared it in a practically quantitative yield by the reaction of stoichiometric amounts of  $(\text{NBU}_4)_2[\text{Cu}(\text{opba})]$ ,  $\text{Mn}(\text{CH}_3\text{COO})_2 \cdot 4\text{H}_2\text{O}$ , and  $(\text{NBU}_4)_2\text{ox}$  in a water/DMSO (1:1 v/v) mixture as solvent.

Apart from the absorptions at 2957, 2918, and 2870  $\text{cm}^{-1}$  that are due to the C—H stretching of the tetra-*n*-butylammonium cation, the most prominent peaks in the IR

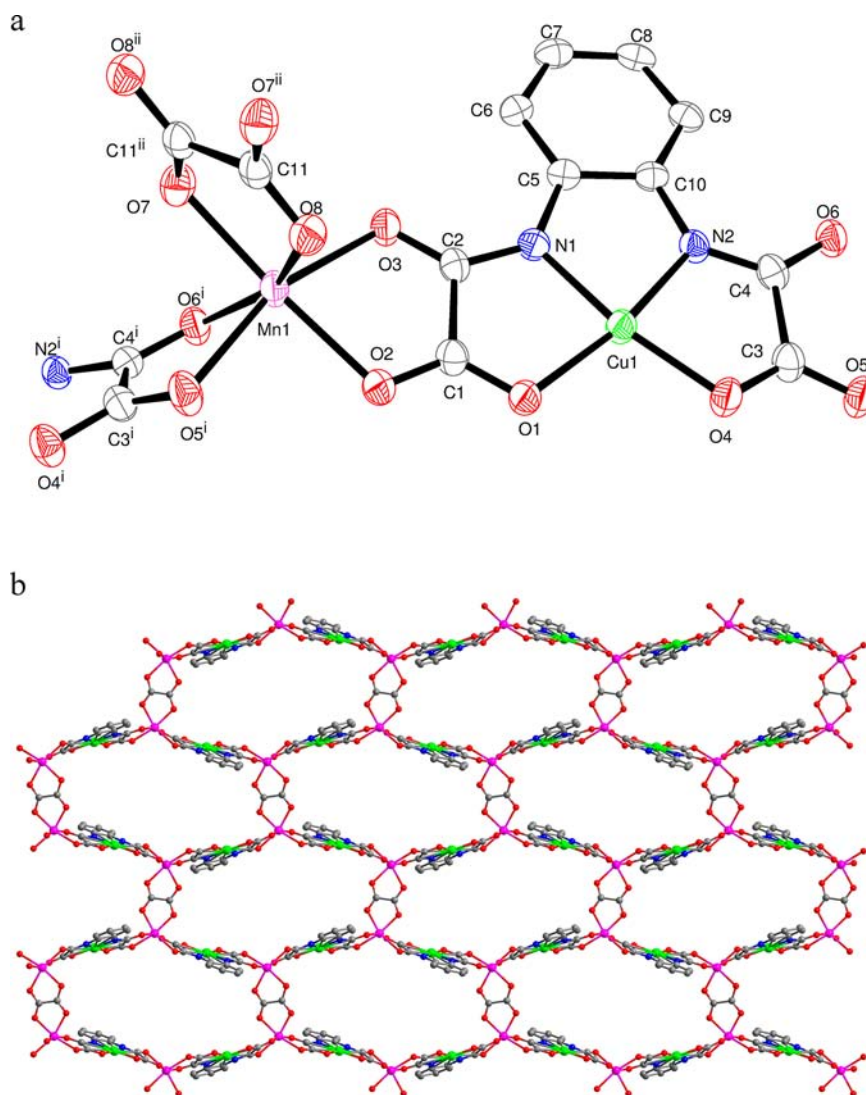


**Figure 1.** (a) View of the crystal structure depicting the metal surroundings in compound **1** with the numbering of the non-hydrogen. Thermal ellipsoids are drawn at the 50% probability level, and the hydrogen atoms are omitted for clarity. (b) View of a fragment of the  $[\text{Mn}\{\text{Cu}(\text{opba})\}_2\text{ox}]_n^{2n-}$  anionic layer extending in the plane (101).

spectrum of **1** are those concerning the presence of the oxalate and opba ligands. The set of the absorptions attributed to the oxalate [ $1682\text{s}$ h and  $1662\text{s}$   $\text{cm}^{-1}$  ( $\nu_{\text{as}}(\text{CO})$ ),  $1355\text{m}$  and  $1312\text{w}$   $\text{cm}^{-1}$  ( $\nu_{\text{s}}(\text{CO})$ ), and  $794\text{m}$   $\text{cm}^{-1}$  ( $\delta(\text{OCO})$ )] supports its presence in a bis-bidentate coordination mode.<sup>35</sup> Finally, the strong absorption at  $1603$   $\text{cm}^{-1}$  and shoulder at  $1623$   $\text{cm}^{-1}$ , which are assigned to the  $\nu_{\text{as}}(\text{CO})$  of the oxamate in **1**, indicate a bis-bidentate coordination mode of the 1,2-phenylenebis(oxamato)cuprate(II) in **1** in comparison with the uncoordinated carbonyl groups in the mononuclear  $(\text{NBU}_4)_2[\text{Cu}(\text{opba})]$  salt (three strong peaks at  $1676$ ,  $1648$ , and  $1614$   $\text{cm}^{-1}$ ).<sup>36</sup>

The thermogravimetric/differential thermal analysis (TG/DTA) data for **1** are given in the Supporting Information (Figure S2). The TGA curve of **1** under  $\text{N}_2$  shows a first mass loss in the temperature range  $21$ – $364$   $^\circ\text{C}$  that has been attributed to the removal of one tetra-*n*-butylammonium cation, half a mole of oxalate, and the phenyl ring of the opba ligand due its partial decomposition [per  $\text{Cu}^{\text{II}}\text{Mn}^{\text{II}}$  pair], corresponding to the mass losses of  $37.05$ ,  $6.73$ , and  $11.63\%$ , respectively (Found:  $56.14\%$ . Calcd:  $55.41\%$ ). Only one endothermic peak is observed in the DTA curve at  $364$   $^\circ\text{C}$ , which is tentatively

attributed to the thermal decomposition of the oxamate group. Its decomposition continues in the second mass loss in the temperature range  $364$ – $750$   $^\circ\text{C}$  (Found:  $20.92\%$ . Theoretical value for  $\text{N}_2\text{C}_4\text{O}_4$ :  $21.44\%$ ) with a final residue of ca.  $22.94\%$ , which essentially contains equimolar amounts of  $\text{MnO}$  and  $\text{CuO}$  (Calcd:  $23.15\%$ ).

**Description of the Structure of 1.** The crystal structure of **1** consists of an anionic two-dimensional network of formula  $[\text{Mn}_2\{\text{Cu}(\text{opba})\}_2\text{ox}]_n^{2n-}$  and tetra-*n*-butylammonium cations (Figure 1). The structure can be viewed as heterobimetallic zigzag chains of  $[\text{MnCu}(\text{opba})]$  bridged by bis-bidentate oxalate groups leading to a  $6^3$ -hcb net topology that is based on fused  $\text{Mn}_6\text{Cu}_4$  decagon rings. These decagon motifs within each layer are elongated along the crystallographic *a* axis. The dimensions of each ring are  $20 \times 11$  Å, defined as the distances between directly opposing manganese atoms of each cycle. The crystal packing can be described as an extended parallel array of anionic layers exhibiting the ABABA trend that are interleaved by the bulky  $n\text{-Bu}_4\text{N}^+$  cations (Figure 2). The stacking direction is not coincident with any of the crystallographic axes (Figure 2a). In Figure 2b, we can see that two tetra-*n*-butylammonium

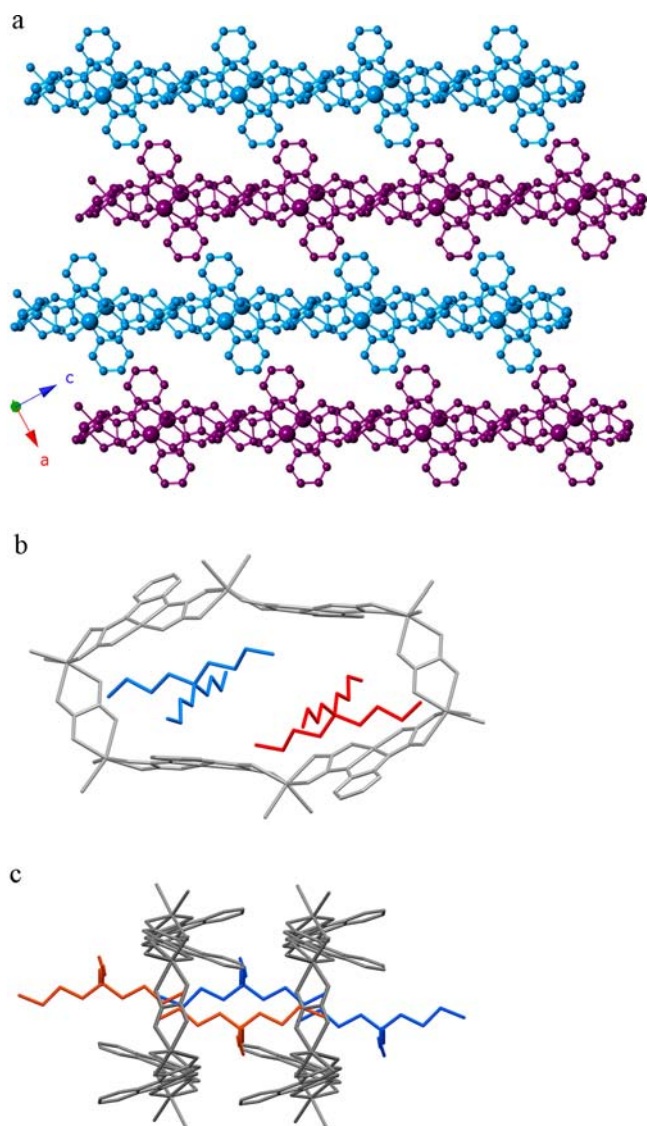


**Figure 2.** (a) View of the ABAB arrangement of the anionic layers in **1**. (b) Top and (c) side views of a Mn<sub>6</sub>Cu<sub>4</sub> decagon unit of **1** showing the location of the tetra-*n*-butylammonium cations.

cations are pointing through a Mn<sub>6</sub>Cu<sub>4</sub> decagon unit of **1**, and Figure 2c reveals the partial penetration of an *n*-butyl group of the cation (two carbon atoms) into the anionic layer.

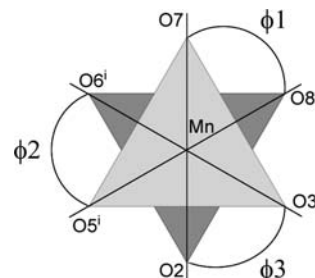
The shortest interlayer metal–metal (Mn(1)⋯Cu(1)<sup>i</sup>) separation is 9.270(1) Å, a value which is much greater than those of the intralayer metal–metal distances [5.389(1), 5.314(1), 5.629(1), and 5.314(1) Å for Cu(1)⋯Mn(1), Mn(1)⋯Cu(1)<sup>ii</sup>, Mn(1)⋯Mn(1)<sup>iii</sup>, and Cu(1)⋯Mn(1)<sup>iv</sup>, respectively; symmetry code: (i) =  $-1+x, y, z$ ; (ii) =  $x-1/2, -y+1/2, z-1/2$ ; (iii) =  $-x+3, -y+1, -z$ ; (iv) =  $x+1/2, -y+1/2, z+1/2$ ]. The values of the Cu(1)⋯Mn(1)⋯Mn(1)<sup>iii</sup>, Cu(1)⋯Mn(1)⋯Cu(1)<sup>ii</sup>, Mn(1)⋯Cu(1)⋯Mn(1)<sup>ii</sup>, and Cu(1)<sup>iii</sup>⋯Mn(1)⋯Mn(1)<sup>iii</sup> angles within each ring are 113.44(1), 147.46(1), 166.80(1), and 96.55(1)°, respectively.

Each Cu<sup>II</sup> ion is four-coordinate in distorted CuN<sub>2</sub>O<sub>2</sub> square planar geometry (Figure 1) with values of the Cu–O [1.960(2) and 1.942(2) Å] and Cu–N [1.917(3) and 1.915(3) Å] bond lengths that agree with those previously reported for other compounds containing the [Cu(opba)]<sup>2-</sup> unit.<sup>9,11a,b,12e,16d</sup> The copper atom is shifted by only 0.0259(14) Å from the

N(1)N(2)O(1)O(4) mean basal plane. The fact that the [Cu(opba)]<sup>2-</sup> unit acts as a bis-bidentate ligand toward two Mn<sup>II</sup> ions causes a geometrical constraint in the fused three five-member chelate rings, which is evidenced by the opening of the less-constrained O(1)–Cu(1)–O(4) angle [105.53(10)°] with respect to the reduced bite values subtended at the copper(II) ion by the chelating opba [82.92(11), 85.12(10), and 85.39(10)° for N(1)–Cu(1)–N(2), N(1)–Cu(1)–O(1), and N(2)–Cu(1)–N(4), respectively].

The Mn<sup>II</sup> ion is in a distorted six-coordinate MnO<sub>6</sub> environment that is built by four oxamate-oxygen atoms from two [Cu(opba)]<sup>2-</sup> units and two oxalate-oxygen atoms. The reduced values of the bite angle of the oxamate [76.71(8) and 76.58(9)° for O(2)–Mn(1)–O(3) and O(5)<sup>i</sup>–Mn(1)–O(6)<sup>i</sup>, respectively] and oxalate [76.96(9)° for O(7)–Mn(1)–O(8)] are the main factors accounting for this distortion. The values of the Mn–O bond distances vary in the narrow range 2.152(2)–2.211(2) Å, and they are in agreement with those observed in previous structures concerning opba-(oxamato-κ<sup>2</sup>O,O')manganese(II) units<sup>9,11a,b,16d</sup> and oxalate-bridged dimanganese(II) compounds.<sup>37</sup> The degree of twist at the tris-chelated Mn(1) atom calculated as the average value of  $\phi_1$  (47.0°),  $\phi_2$  (35.0°), and  $\phi_3$  (44.6°) (Scheme 2) is 42.2° ( $\phi = 0$

**Scheme 2.** Twisting of the Tris-Chelating Manganese(II) Environment



and 60° for an ideal trigonal prism and octahedron, respectively). This distortion of the octahedral ( $O_h$ ) metal environment toward trigonal prismatic ( $D_{3h}$ ), a so-called Bailar twist,<sup>38</sup> is explained by the small values of the bite angles from the chelating oxamate/oxalate groups. In such surroundings, the manganese(II) ion occupies a chiral site, but each ring in the structure shows a perfect alternance of  $\Delta$  and  $\Lambda$  chiral sites, as shown in Figure 3. As these sites are not strictly related by a mirror plane, it would not be correct to refer to it as a racemic composition.

The oxalate ligand is planar; the value of its carbon–carbon bond length [1.566(6) Å for C(11)–C(11)<sup>iii</sup>] and O(7)–C(11)–O(8) bond angles [126.3(3)°] agree with those expected for a single C–C bond and sp<sup>2</sup> hybridization,

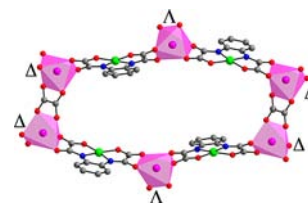


**Figure 3.** Representation of a Mn<sub>6</sub>Cu<sub>4</sub> decagon cycle from **1** showing the alternating  $\Delta$  and  $\Lambda$  enantiomeric forms of the tris-chelated manganese(II) ion.

respectively. The values of the dihedral angles between the oxalate [C(11)O(7)O(8)C(11)<sup>iii</sup>O(7)<sup>iii</sup>O(8)<sup>iii</sup>] set of atoms] and the mean planes of the two oxamate groups [O(11)C(1)-O(2)C(2)N(1)O(3)N(2)C(4)O(6)C(3)O(4)O(5)] and O(11)<sup>ii</sup>C(1)<sup>ii</sup>O(2)<sup>ii</sup>C(2)<sup>ii</sup>N(1)<sup>ii</sup>O(3)<sup>ii</sup>N(2)<sup>ii</sup>C(4)<sup>ii</sup>O(6)<sup>ii</sup>C(3)<sup>ii</sup>O(4)<sup>ii</sup>O(5)<sup>ii</sup>] around the Mn(1) are 72.46(9) and 88.28 (9)°, respectively, whereas that between the two oxamate mean planes is 45.93(3)°. The manganese(II) ion belongs to the plane of the oxalate ligand, but it is shifted by 0.034(4) and 0.280(2) Å from the O(1)O(2)O(3)N(1)C(1)C(2) and O(4)O(5)O(6)N(2)C(3)C(4) mean planes. The phenylene ring of the opba<sup>4-</sup> ligand is planar, and it is practically coplanar with the equatorial plane defined by the N(1)N(2)O(1)O(4) set of atoms. The C(1)–C(2) and C(3)–C(4) bond distances of the oxamate fragments are 1.558(5) and 1.549(5) Å, respectively, values which agree with those expected for a single C–C bond. The tetra-*n*-butylammonium cations adopt the usual tetrahedral shape, and they are located between the anionic layers with two butyl substituents pointing toward the decagon holes of two neighboring layers, and the other two butyl arms are parallel to the layers [Figure 2 Parts b and c]. This partial occupation of the holes of the decagon cycles by the countercations in **1** accounts for the lack of guest solvent molecules in the structure. Finally, it is interesting to point out that the NBu<sub>4</sub><sup>+</sup> cation has been used as a templating agent for the preparation of two-dimensional oxalate-bridged bimetallic anionic networks.<sup>39</sup>

**Magnetic Properties of 1.** The magnetic properties of **1** in the form of  $\chi_M T$  vs  $T$  plot ( $\chi_M$  is the magnetic susceptibility per Cu<sup>II</sup>Mn<sup>II</sup> unit) are shown in Figure 4.  $\chi_M T$  at 300 K is equal to

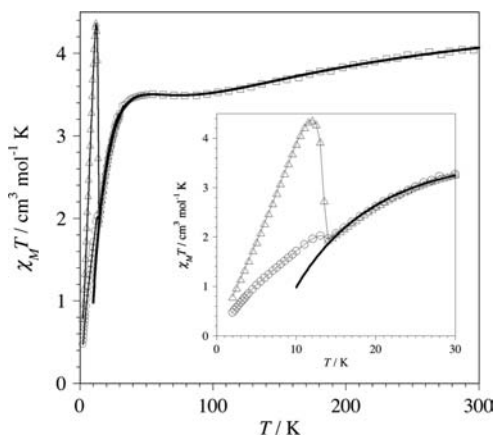


**Figure 4.** Thermal dependence of  $\chi_M T$  for **1** under applied dc fields of 3000 G ( $\square$ ), 500 G ( $\circ$ ), and 50 G ( $\triangle$ ). The broad solid line is the best-fit curve (see text), whereas the thinner line is only an eye-guide. The inset shows more detail in the low temperature region.

$4.03 \text{ cm}^3 \text{ mol}^{-1}$ , a value which is somewhat below the calculated one for the sum of a square planar copper(II) ion and a octahedral high-spin manganese(II) ion ( $\chi_M T = 4.75 \text{ cm}^3 \text{ mol}^{-1} \text{ K}$  with  $g_{\text{Mn}} = g_{\text{Cu}} = 2.0$ ). Upon cooling,  $\chi_M T$  continuously decreases to attain a plateau of  $3.50 \text{ cm}^3 \text{ mol}^{-1} \text{ K}$  in the temperature range 80–45 K, and then it sharply decreases to attain a minimum of  $1.97 \text{ cm}^3 \text{ mol}^{-1} \text{ K}$  at 14.0 K, which is followed by an abrupt increase at lower temperatures. This increase is field dependent as shown in the inset of Figure 4. Two conclusions can be extracted from these features: (i) the presence of important antiferromagnetic interactions between the paramagnetic centers supported by the fact that the values

of  $\chi_M T$  at the plateau and at the minimum are well below that of a magnetically isolated manganese(II) ion and (ii) the occurrence of spin canting which is responsible for the increase of  $\chi_M T$  at very low temperatures the value of the magnetic ordering being at  $T_c$  ca. 14 K, as seen in the field cooled (FC) magnetization curve (see Figure 5).

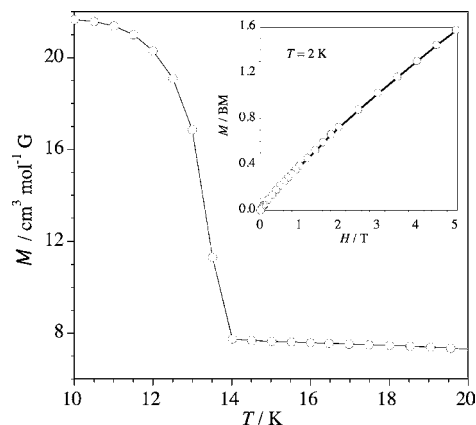


**Figure 5.** Thermal dependence of the field-cooled magnetization under an applied dc field of 50 G. The inset shows the magnetization versus  $H$  plot for **1** at 2.0 K.

Concerning the first conclusion, there are two intralayer exchange pathways in **1** that correspond to the oxamate-bridged Cu<sup>II</sup>Mn<sup>II</sup> and oxalato-bridged Mn<sup>II</sup>Mn<sup>II</sup> motifs. When the previous magneto-structural investigations on these two motifs are considered, the first one is much more efficient as mediator of magnetic interactions than the second one; the values of  $-J_{\text{Cu}^{\text{II}}\text{Mn}^{\text{II}}}$  through the oxamate vary in the range  $25.2\text{--}35.2 \text{ cm}^{-1}$ ,<sup>11a,14c,16c,17,18c</sup> whereas those of  $-J_{\text{Mn}^{\text{II}}\text{Mn}^{\text{II}}}$  across the bis-bidentate oxalato cover the range  $1.7\text{--}3.0 \text{ cm}^{-1}$ .<sup>37</sup> Therefore, the decrease of the  $\chi_M T$  product in the high temperature domain of Figure 4 obeys the oxamate pathway, whereas the subsequent plateau of  $\chi_M T$  would be caused by the compensation between the expected increase of  $\chi_M T$  after attaining the minimum, which is characteristic for any ferrimagnetic Cu<sup>II</sup>Mn<sup>II</sup> chain,<sup>11a,16c,17</sup> and the decrease of  $\chi_M T$  is due to the interchain Mn<sup>II</sup>–( $\mu$ -oxalato)–Mn<sup>II</sup> pathway. This last one can lead to the cancellation of the spins between the ferrimagnetic chains and then to a vanishing  $\chi_M T$  at low temperatures. There is no theoretical model to analyze the magnetic data of **1**. However, its magnetic data from room temperature to 16 K were successfully reproduced through quantum Monte Carlo (QMC) simulations by using the manganese(II)–copper(II)  $6^3\text{-hcb}$  two-dimensional structural model. The best-fit data are  $g_{\text{Mn}} = 2.000(3)$ ,  $g_{\text{Cu}} = 2.018(3)$ ,  $J_{\text{CuMn}} = -32.5(3) \text{ cm}^{-1}$ , and  $J_{\text{MnMn}} = -2.7(3) \text{ cm}^{-1}$ . The agreement factor, defined as  $F = \sum [(\chi_M T)_{\text{exp}} - (\chi_M T)_{\text{calc}}]^2 / \sum [(\chi_M T)_{\text{exp}}]^2$ , was  $1.3 \times 10^{-5}$ . The values of the magnetic coupling obtained compare well with those already reported for these exchange pathways in other, simpler compounds, a feature that strongly supports the validity of the computational methodology that we have used to analyze the magnetic data of **1**.

As far as the spin canting in **1** is concerned, the lack of hysteresis loop in the magnetization vs  $H$  plot at 2.0 K (see inset of Figure 5) may be due to a small hysteresis, in agreement with the very weak value of the remnant magnetization,  $M_r$  ca.  $0.004 \mu_B$ . The roughly estimated value

of the canting angle ( $\alpha$ ) through the expression  $\sin \alpha = M_r/gM_S$  with  $g = 2$  and  $M_S = 2$  is ca.  $0.001^\circ$ . This very weak spin canting in **1** is in agreement with the quasi-isotropic character of the interacting copper(II) and manganese(II) ions, a phenomenon that most commonly occurs in magnetic systems with anisotropic transition metal ions.<sup>40–42</sup> When the anisotropy of the local spins is very low, as in the case of Fe(III) for instance, the spin canting has its origin in the antisymmetric exchange.<sup>43,44</sup> However, ions with magnetic moments in a unit cell cannot be related by a center of symmetry if canting is to occur through this mechanism. Given that compound **1** crystallizes in a centrosymmetric space group, the canting observed is in conflict with the antisymmetric exchange. A small structural distortion (phase transition) at very low temperatures in **1** could break its inversion center, making possible the occurrence of the canting observed below  $T_c$ .

## CONCLUDING REMARKS

In conclusion, we have prepared a new spin-canted heterobimetallic 2-D network of formula  $(\text{Bu}_4\text{N})_2[\text{Mn}_2\{\text{Cu}(\text{opba})_2\text{ox}]$  (**1**), representing a unique example of a layered system containing copper(II) and manganese(II) ions bridged by oxamate and oxalate groups. It is worth noting that it is the first time that single-crystal X-ray structure determination has been accomplished for the two-dimensional oxamato-based magnets of general formula  $(\text{cation})_2[\text{M}_2\{\text{Cu}(\text{opba})_2\}]$ . Compound **1** can also become the first example of a new family of layered heterobimetallic compounds that can be prepared taking advantage of the templating effect of the tetralkylammonium derivatives. Finally, the intralayer antiferromagnetic interactions in the complex spin topology of **1** were evaluated through the analysis of the magnetic susceptibility data by the use of the QMC methodology.

## ASSOCIATED CONTENT

### Supporting Information

PXRD data (Figure S1) and thermal behavior (Figure S2) of **1**. This material is available free of charge via the Internet at <http://pubs.acs.org>. CCDC 923163 contains the X-ray crystallographic data of **1** in a CIF file.

## AUTHOR INFORMATION

### Corresponding Author

\*E-mail: H.O.S, [stumpf@ufmg.br](mailto:stumpf@ufmg.br); M.J., [miguel.julve@uv.es](mailto:miguel.julve@uv.es).

### Notes

The authors declare no competing financial interest.

## ACKNOWLEDGMENTS

The authors thank the Conselho Nacional de Desenvolvimento Científico e Tecnológico (CNPq), the Fundação de Amparo à Pesquisa do Estado de Minas Gerais (FAPEMIG), the Coordenação de Aperfeiçoamento de Pessoal de Nível Superior (CAPES), and the Ministerio Español de Ciencia e Innovación (Projects CTQ2010-15364, MAT2010-19681, and HB2012-0290). H.O.S. acknowledges the University of Valencia for a Visiting Professorship.

## REFERENCES

(1) (a) Kahn, O. *Struct. Bonding (Berlin, Ger.)* **1987**, *68*, 89. (b) Kahn, O. *Adv. Inorg. Chem.* **1995**, *43*, 179.

(2) Pardo, E.; Ruiz-García, R.; Cano, J.; Ottenwaelder, X.; Lescouëzec, R.; Journaux, Y.; Lloret, F.; Julve, M. *Dalton Trans.* **2008**, 2780.

(3) Dul, M. C.; Pardo, E.; Lescouëzec, R.; Journaux, Y.; Ferrando-Soria, J.; Ruiz-García, R.; Cano, J.; Julve, M.; Lloret, F.; Cangussu, D.; Pereira, C. L. M.; Stumpf, H. O.; Pasán, J.; Ruiz-Pérez, C. *Coord. Chem. Rev.* **2010**, *254*, 2281.

(4) Ruiz, R.; Faus, J.; Lloret, F.; Julve, M.; Journaux, Y. *Coord. Chem. Rev.* **1999**, *193–195*, 1069.

(5) (a) van Koningsbruggen, P. J.; Kahn, O.; Nakatani, K.; Pei, Y.; Renard, J. P.; Drillon, M.; Legoll, P. *Inorg. Chem.* **1990**, *29*, 3325.

(b) Kahn, O.; Stumpf, H.; Pei, Y.; Sletten, J. *Mol. Cryst. Liq. Cryst.* **1993**, *233*, 231. (c) Gulbrandsen, A.; Sletten, J.; Nakatani, K.; Pei, Y.; Kahn, O. *Inorg. Chim. Acta* **1993**, *212*, 271. (d) Lloret, F.; Julve, M.; Ruiz, R.; Nakatani, K.; Kahn, O.; Sletten, J. *Inorg. Chem.* **1993**, *32*, 27.

(6) (a) Tercero, J.; Díaz, C.; Salah El Fallah, M.; Mahía, J. *Inorg. Chem.* **2001**, *40*, 3077. (b) Tercero, J.; Díaz, C.; Ribas, J.; Mahía, J.; Maestro, M.; Solans, X. *J. Chem. Soc., Dalton Trans.* **2002**, 2040. (c) Tercero, J.; Díaz, C.; Ribas, J.; Mahía, J.; Maestro, M. A. *Inorg. Chem.* **2002**, *41*, 5373. (d) Tercero, J.; Díaz, C.; Ribas, J.; Maestro, M.; Mahía, J.; Stoeckli-Evans, H. *Inorg. Chem.* **2003**, *42*, 3366.

(7) Benelli, C.; Fabretti, A. C.; Giusti, A. *J. Chem. Soc., Dalton Trans.* **1993**, 409.

(8) Zhang, L.; Wang, S. B.; Yang, G. M.; Tang, J. K.; Liao, D. Z.; Jiang, Z. H.; Yan, S. P.; Cheng, P. *Inorg. Chem.* **2003**, *42*, 1462.

(9) Neels, A.; Stoeckli-Evans, H.; Chavan, S. A.; Yakhmi, J. V. *Inorg. Chim. Acta* **2001**, *326*, 106.

(10) (a) Rüffer, T.; Bräuer, B.; Powell, A. K.; Hewitt, I.; Salvan, G. *Inorg. Chim. Acta* **2007**, *360*, 3475. (b) Rüffer, T.; Bräuer, B.; Meva, F. E.; Walfort, B.; Salvan, G.; Powell, A. K.; Hewitt, I. J.; Sorace, L.; Caneschi, A. *Inorg. Chim. Acta* **2007**, *360*, 3777. (c) Rüffer, T.; Bräuer, B.; Meva, F. E.; Sorace, L. *Inorg. Chim. Acta* **2009**, *362*, 563.

(11) (a) Stumpf, H. O.; Pei, Y.; Kahn, O.; Sletten, J.; Renard, J. P. *J. Am. Chem. Soc.* **1993**, *115*, 6738. (b) Stumpf, H. O.; Ouahab, L.; Pei, Y.; Grandjean, D.; Kahn, O. *Science* **1993**, *261*, 447. (c) Vaz, M. G. F.; Pedroso, E. F.; Speziali, N. L.; Novak, M. A.; Alcântara, A. F. C.; Stumpf, H. O. *Inorg. Chim. Acta* **2001**, *326*, 65. (d) Cador, O.; Vaz, M. G. F.; Stumpf, H. O.; Mathonière, C. *J. Magn. Magn. Mater.* **2001**, *234*, 6. (e) Vaz, M. G. F.; Knobel, M.; Speziali, N. L.; Moreira, A. M.; Alcântara, A. F. C.; Stumpf, H. O. *J. Braz. Chem. Soc.* **2002**, *13*, 183. (f) Pereira, C. L. M.; Pedroso, E. F.; Stumpf, H. O.; Novak, M. A.; Ricard, L.; Ruiz-García, R.; Rivière, E.; Journaux, Y. *Angew. Chem., Int. Ed.* **2004**, *43*, 956. (g) Pereira, C. L. M.; Pedroso, E. F.; Doriguetto, A. C.; Ellena, J. A.; Boubekeur, K.; Filali, Y.; Journaux, Y.; Novak, M. A.; Stumpf, H. O. *Dalton Trans.* **2011**, *40*, 746.

(12) (a) Pardo, E.; Ruiz-García, R.; Lloret, F.; Julve, M.; Cano, J.; Pasán, J.; Ruiz-Pérez, C.; Filali, Y.; Chamoreau, L. M.; Journaux, Y. *Inorg. Chem.* **2007**, *46*, 4504. (b) Pardo, E.; Cangussu, D.; Lescouëzec, R.; Journaux, Y.; Pasán, J.; Delgado, F. S.; Ruiz-Pérez, C.; Ruiz-García, R.; Cano, J.; Julve, M.; Lloret, F. *Inorg. Chem.* **2009**, *48*, 4661. (c) Dul, M. C.; Ottenwaelder, X.; Pardo, E.; Lescouëzec, R.; Journaux, Y.; Chamoreau, L. M.; Ruiz-García, R.; Cano, J.; Julve, M.; Lloret, F. *Inorg. Chem.* **2009**, *48*, 5244. (d) Ferrando-Soria, J.; Pasán, J.; Ruiz-Pérez, C.; Journaux, Y.; Julve, M.; Lloret, F.; Cano, J.; Julve, M. *Inorg. Chem.* **2011**, *50*, 8694. (e) Simões, T. R. G.; Mambri, R. V.; Reis, D. O.; Marinho, M. V.; Ribeiro, M. A.; Pinheiro, C. B.; Ferrando-Soria, J.; Déniz, M.; Ruiz-Pérez, C.; Cangussu, D.; Stumpf, H. O.; Lloret, F.; Julve, M. *Dalton Trans.* **2013**, *42*, 5778.

(13) (a) Verdager, M.; Kahn, O.; Julve, M.; Gleizes, A. *Nouv. J. Chim.* **1985**, *9*, 325. (b) Cano, J.; Ruiz, E.; Alemany, P.; Lloret, F.; Alvarez, S. *J. Chem. Soc., Dalton Trans.* **1999**, 1669.

(14) (a) Pardo, E.; Carrasco, R.; Ruiz-García, R.; Julve, M.; Lloret, F.; Muñoz, M. C.; Journaux, Y.; Ruiz, E.; Cano, J. *J. Am. Chem. Soc.* **2008**, *130*, 576. (b) Pardo, E.; Train, C.; Lescouëzec, R.; Journaux, Y.; Pasán, J.; Ruiz-Pérez, C.; Delgado, F. S.; Ruiz-García, R.; Lloret, F.; Paulsen, C. *Chem. Commun.* **2010**, *46*, 2322. (c) Ferrando-Soria, J.; Cangussu, D.; Eslava, M.; Journaux, Y.; Lescouëzec, R.; Julve, M.; Lloret, F.; Pasán, J.; Ruiz-Pérez, C.; Lhotel, E.; Paulsen, C.; Pardo, E. *Chem.—Eur. J.* **2011**, *17*, 12482. (d) Ferrando-Soria, J.; Ruiz-García, R.; Cano,

- J.; Stiriba, S. E.; Vallejo, J.; Castro, I.; Julve, M.; Lloret, F.; Amorós, P.; Pasán, J.; Ruiz-Pérez, C.; Journaux, Y.; Pardo, E. *Chem.—Eur. J.* **2012**, *18*, 1608. (e) Ferrando-Soria, J.; Serra-Crespo, P.; Lange, M.; Gascon, J.; Kapteijn, F.; Julve, M.; Cano, J.; Lloret, F.; Pasán, J.; Ruiz-Pérez, C.; Journaux, Y.; Pardo, E. *J. Am. Chem. Soc.* **2012**, *134*, 15301. (f) Ferrando-Soria, J.; Khajavi, H.; Serra-Crespo, P.; Gascon, J.; Kapteijn, F.; Julve, M.; Lloret, F.; Pasán, J.; Ruiz-Pérez, C.; Journaux, Y.; Pardo, E. *Adv. Mater.* **2012**, *24*, 5625.
- (15) Pei, Y.; Verdaguier, M.; Kahn, O. *J. Am. Chem. Soc.* **1986**, *108*, 7428.
- (16) (a) Pei, Y.; Verdaguier, M.; Kahn, O.; Sletten, J.; Renard, J. P. *Inorg. Chem.* **1987**, *26*, 138. (b) Pei, Y.; Kahn, O.; Sletten, J.; Renard, J. P.; Georges, R.; Gianduzzo, J. C.; Curély, J.; Xu, Q. *Inorg. Chem.* **1988**, *27*, 47. (c) Nakatani, K.; Bergerat, P.; Codjovi, E.; Mathonière, C.; Pei, Y.; Kahn, O. *Inorg. Chem.* **1991**, *30*, 3977. (d) Sumpf, H. O.; Pei, Y.; Ouahab, L.; Le Berre, F.; Codjovi, E.; Kahn, O. *Inorg. Chem.* **1993**, *32*, 5687. (e) Larionova, J.; Chavan, S. A.; Yakhmi, J. V.; Frøystein, A. G.; Sletten, J.; Sourisseau, C.; Kahn, O. *Inorg. Chem.* **1997**, *36*, 6374.
- (17) Pereira, C. L. M.; Dorignetto, A.; Konzen, C. C.; Meira-Belo, L. C.; Leitao, U. A.; Fernandes, N. G.; Mascarenhas, Y. P.; Ellena, J.; Brandl, A. L.; Knobel, M.; Stumpf, H. O. *Eur. J. Inorg. Chem.* **2005**, 5018.
- (18) (a) Pardo, E.; Ruiz-García, R.; Lloret, F.; Faus, J.; Julve, M.; Journaux, Y.; Delgado, F. S.; Ruiz-Pérez, C.; Muñoz, M. C. *Adv. Mater.* **2004**, *16*, 1597. (b) Pardo, E.; Ruiz-García, R.; Lloret, F.; Faus, J.; Julve, M.; Journaux, Y.; Novak, M. A.; Delgado, F. S.; Ruiz-Pérez, C. *Chem.—Eur. J.* **2007**, *13*, 2054. (c) Ferrando-Soria, J.; Pardo, E.; Ruiz-García, R.; Cano, J.; Lloret, F.; Julve, M.; Journaux, Y.; Pasán, J.; Ruiz-Pérez, C. *Chem.—Eur. J.* **2011**, *17*, 2176.
- (19) Oliveira, W. X. C.; Ribeiro, M. A.; Pinheiro, C. B.; Nunes, W. C.; Julve, M.; Journaux, Y.; Stumpf, H. O.; Pereira, C. L. M. *Eur. J. Inorg. Chem.* **2012**, 5685.
- (20) (a) Cadot, O.; Price, D.; Larionova, J.; Mathonière, C.; Kahn, O.; Yakhmi, J. V. *J. Mater. Chem.* **1997**, *7*, 1263. (b) Dias, M. C.; Knobel, M.; Stumpf, H. O. *J. Magn. Magn. Mater.* **2001**, *226*, 1961.
- (21) Daiguebonne, C.; Guillou, O.; Kahn, M. L.; Kahn, O.; Oushoorn, R. L.; Boubekeur, K. *Inorg. Chem.* **2001**, *40*, 176.
- (22) Oushoorn, R. L.; Boubekeur, K.; Batail, P.; Guillou, O.; Kahn, O. *Bull. Soc. Chim. Fr.* **1996**, 133, 77.
- (23) Kahn, M. L.; Mathonière, C.; Kahn, O. *Inorg. Chem.* **1999**, *38*, 3692.
- (24) Kerbellec, N.; Mahé, N.; Guillou, O.; Daiguebonne, C.; Cadot, O.; Roisnel, T.; Oushoorn, R. L. *Inorg. Chim. Acta* **2005**, *358*, 3246.
- (25) Earnshaw, A. *Introduction to Magnetochemistry*; Academic Press: London, 1968.
- (26) Homma, S.; Matuda, H.; Ogita, N. *Prog. Theor. Phys.* **1986**, *75*, 1058.
- (27) Miyazawa, S.; Miyashita, S.; Makivic, M. S.; Homma, M. S. *Prog. Theor. Phys.* **1993**, *89*, 1167.
- (28) *Crysalis PRO*; Agilent Technologies UK Ltd.: Yarnton, England, 2011.
- (29) Sheldrick, G. M. *Acta Crystallogr.* **2008**, *A64*, 112.
- (30) Johnson, C. K. In *Crystallographic Computing*; Ahmed, F. R., Ed.; Munksgaard: Copenhagen, Denmark, 1970; p 207–219.
- (31) Platon: Spek, A. L. *Acta Crystallogr.* **2009**, *D65*, 148.
- (32) (a) Brandenburg, K.; Putz, H. *DIAMOND 2.1d*; Crystal Impact: Bonn, Germany, 2000. (b) Macrae, F.; Edgington, P. R.; McCabe, P.; Pidcock, E.; Shields, G. P.; Taylor, R.; Towler, M.; van der Streek, J. J. *Appl. Crystallogr.* **2006**, *39*, 453.
- (33) (a) Soto, L.; García, J.; Escrivá, E.; Legros, J. P.; Tuchagues, J. P.; Dahan, F.; Fuertes, A. *Inorg. Chem.* **1989**, *28*, 3378. (b) Dey, S.; Sarkar, S.; Mukherjee, T.; Mondal, B.; Zangrando, E.; Sutter, J. P.; Chattopadhyay, P. *Inorg. Chim. Acta* **2011**, *376*, 129. (c) Vilela, R. S.; Oliveira, T. L.; Martins, F. T.; Ellena, J. A.; Lloret, F.; Julve, M.; Cangussu, D. C. R. *Chim.* **2012**, *15*, 856.
- (34) (a) Oxamide can be converted to ammonium oxalate and oxalic acid by heating it for long periods with water; the best results are obtained under pressure. See: Riemenschneider, W.; Tanifuji, M. *Oxalic Acid*. In *Ullmann's Encyclopedia of Industrial Chemistry*; Wiley-VCH: Weinheim, Germany, 2000. (b) Du, M.; Zhang, Z.-H.; Li, C.-P.; Ribas-Ariño, J.; Aliaga-Alcalde, N.; Ribas, J. *Inorg. Chem.* **2011**, *50*, 6850.
- (35) De Munno, G.; Armentano, D.; Julve, M.; Lescouëzec, R.; Faus, J. *Inorg. Chem.* **1999**, *38*, 2234.
- (36) Cangussu, D.; Nunes, W. C.; Pereira, C. L. M.; Pedroso, E. F.; Mazali, I. O.; Knobel, M.; Alves, O. L.; Stumpf, H. O. *Eur. J. Inorg. Chem.* **2008**, 3802.
- (37) (a) De Munno, G.; Ruiz, R.; Lloret, F.; Faus, J.; Sessoli, R.; Julve, M. *Inorg. Chem.* **1995**, *34*, 408. (b) Glerup, J.; Goodson, P. A.; Hodgson, D. J.; Michelsen, K. *Inorg. Chem.* **1995**, *34*, 6255. (c) Marinescu, G.; Andruh, M.; Lescouëzec, R.; Muñoz, M. C.; Cano, J.; Lloret, F.; Julve, M. *New J. Chem.* **2000**, *24*, 527. (d) García-Couceiro, U.; Olea, D.; Castillo, O.; Luque, A.; Román, P.; De Pablo, P. J.; Gómez-Herrero, J.; Zamora, F. *Inorg. Chem.* **2005**, *44*, 8343. (e) Fuller, A. L.; Watkins, R. W.; Dunbar, K. R.; Prosvirin, A. V.; Arif, A. M.; Berreau, L. M. *Dalton Trans.* **2005**, 1891. (f) García-Terán, J. P.; Castillo, O.; Luque, A.; García-Couceiro, U.; Beobide, G.; Román, P. *Dalton Trans.* **2006**, 902. (g) García-Couceiro, U.; Castillo, O.; Cepeda, J.; Luque, A.; Pérez-Yáñez, S.; Román, P. *Inorg. Chim. Acta* **2009**, 4212. (h) Keene, T. D.; Zimmermann, I.; Neels, A.; Sereda, O.; Hauser, J.; Bonin, M.; Hursthouse, M. B.; Price, D. J.; Decurtins, S. *Dalton Trans.* **2010**, 39, 4937.
- (38) Alvarez, S.; Avnir, D.; Lluell, M.; Pinskyce, M. *New J. Chem.* **2002**, *26*, 996.
- (39) (a) Atomyan, L. O.; Shilov, G. V.; Lyubovskaya, R. N.; Zhilyaeva, E. I.; Ovanesyan, N. S.; Pirumova, S. I.; Gusakovskaya, I. G.; Morozov, Y. G. *JETP Lett.* **1993**, *58*, 766. (b) Carling, S. G.; Mathonière, C.; Day, P.; Abdul Malik, K. M.; Coles, S. J.; Hursthouse, M. B. *J. Chem. Soc., Dalton Trans.* **1996**, 1839. (c) Pellaux, R.; Schmale, H. W.; Huber, R.; Fischer, P.; Hauss, T.; Ouladfi, B.; Decurtins, S. *Inorg. Chem.* **1997**, *36*, 2301. (d) Rochon, F. D.; Massarweh, G. *Can. J. Chem.* **1999**, *77*, 2059. (e) Andrés, R.; Gruselle, M.; Malézieux, B.; Verdaguier, M.; Vaissermann, J. *Inorg. Chem.* **1999**, *38*, 4637.
- (40) (a) Chiozzzone, R.; González, R.; Kremer, C.; Cerdá, M. F.; Armentano, D.; De Munno, G.; Martínez-Lillo, J.; Faus, J. *Dalton Trans.* **2007**, 653. (b) González, R.; Barboza, N.; Chiozzzone, R.; Kremer, C.; Armentano, D.; De Munno, G.; Faus, J. *Inorg. Chim. Acta* **2008**, *361*, 2715. (c) Martínez-Lillo, J.; Lloret, F.; Julve, M.; Faus, J. *J. Coord. Chem.* **2009**, *62*, 92. (d) González, R.; Acosta, A.; Chiozzzone, R.; Kremer, C.; Armentano, D.; De Munno, G.; Julve, M.; Lloret, F.; Faus, J. *Inorg. Chem.* **2012**, *51*, 5737. (e) Mousavi, M.; Béreau, V.; Duhayon, C.; Sutter, J. P. C. R. *Chim.* **2012**, *15*, 924. (f) Martínez-Lillo, J.; Armentano, D.; De Munno, G.; Julve, M.; Lloret, F.; Faus, J. *Dalton Trans.* **2013**, 42, 1687.
- (41) (a) Huang, Y. G.; Yuan, D. Q.; Pan, L.; Jiang, F. L.; Wu, M. Y.; Zhang, X. D.; Wei, W.; Gao, Q.; Lee, J. Y.; Li, J.; Hong, M. C. *Inorg. Chem.* **2007**, *46*, 9609. (b) Marino, N.; Mastropietro, T. F.; Armentano, D.; De Munno, G.; Doyle, R. P.; Lloret, F.; Julve, M. *Dalton Trans.* **2008**, 5152. (c) Rodríguez-Diéguez, A.; Seco, J. M.; Colacio, E. *Eur. J. Inorg. Chem.* **2012**, 203.
- (42) Bernot, K.; Luzon, J.; Sessoli, R.; Vindigni, A.; Thion, J.; Richeter, S.; Leclercq, D.; Larionova, J.; van der Lee, A. *J. Am. Chem. Soc.* **2008**, *130*, 1619.
- (43) (a) Dzyaloshinsky, I. *J. Phys. Chem. Solids* **1958**, *4*, 241. (b) Moriya, T. *Phys. Rev.* **1960**, *117*, 635.
- (44) (a) Armentano, D.; De Munno, G.; Lloret, F.; Palii, A. V.; Julve, M. *Inorg. Chem.* **2002**, *41*, 2007. (b) Armentano, D.; De Munno, G.; Mastropietro, T. F.; Proserpio, D. M.; Julve, M.; Lloret, F. *Inorg. Chem.* **2004**, *43*, 5177. (c) Armentano, D.; De Munno, G.; Mastropietro, T. F.; Julve, M.; Lloret, F. *Chem. Commun.* **2004**, 1160. (d) Armentano, D.; Mastropietro, T. F.; De Munno, G.; Rossi, P.; Lloret, F.; Julve, M. *Inorg. Chem.* **2008**, *47*, 3772. (e) Armentano, D.; Mastropietro, T. F.; De Munno, G.; Julve, M.; Lloret, F. *J. Am. Chem. Soc.* **2005**, *127*, 10778.